PROCEEDINGS OF SCIENCE

Parton distribution functions at LO, NLO and NNLO with correlated uncertainties between orders

Mykhailo LISOVYI*
DESY
E-mail: mlisovyi@mail.desy.de

HERAFitter developers' team

Sets of parton distribution functions (PDFs) of the proton are reported for the leading (LO), next-to-leading (NLO) and next-to-next-to leading order (NNLO) QCD calculations. The parton distribution functions are determined with the HERAFitter program using the data from the HERA experiments and preserving correlations between uncertainties for the LO, NLO and NNLO PDF sets. The sets are used to study cross-section ratios and their uncertainties when calculated at different orders in QCD. A reduction of the overall theoretical uncertainty is observed if correlations between the PDF sets are taken into account for the ratio of W^+W^- di-boson to Z boson production cross sections at the LHC.

XXII. International Workshop on Deep-Inelastic Scattering and Related Subjects
28 April - 2 May 2014
Warsaw, Poland

*Speaker.

PoS(DIS2014)044

1. Introduction

Accurate knowledge of the parton distribution functions (PDFs) of the proton is required for precision physics at the LHC. PDF sets are now available as determined by several groups at leading-order (LO), next-to-leading-order (NLO) and next-to-next-to-leading-order (NNLO) accuracy in QCD. To obtain the cross-section predictions, the PDF sets should be paired with calculations of the coefficient functions at the matching order of the accuracy. Theoretical uncertainties for the predictions arise from both the PDF and coefficient-function uncertainties.

Most of the Standard Model processes at the LHC are calculated to NLO accuracy. The uncertainties due to missing higher orders for the coefficient functions are typically determined by varying factorisation and renormalisation scales. This leads to uncertainties often as large as 10% of predicted cross sections, which usually exceed uncertainties due to the PDFs determination. For a handful of processes known at NNLO, the PDF uncertainties often exceed uncertainties due to missing higher orders in coefficient-function calculations.

The experimental precision achieved by the LHC experiments often exceeds the precision of theoretical calculations. Ultimately, a more complete set of NNLO calculations should remedy the situation in future. At present, special methods are employed to reduce theoretical uncertainties. One such method is to measure ratios of observables which are expected to have similar higher-order corrections. However, this cancellation is not always possible. For example, the measurement of the W^+W^- di-boson[1] to Z boson production cross-section ratio performed by the CMS collaboration using $\sqrt{s} = 7\,\text{TeV}$ data [1] benefits from cancellation of the PDF uncertainties, but the scale uncertainties for the NLO calculation dominate the theoretical uncertainty. While there is no complete NNLO calculation of the WW production available at present, a reduction of the scale uncertainty for this ratio could be achieved by using NNLO calculations for the Z boson production cross section. To benefit from cancellation of the PDF uncertainties, correlated sets at NLO and NNLO are required in this case.

The paper [2] reports a determination of the PDFs with correlated uncertainties for LO, NLO and NNLO sets. The sets were determined using the data from the HERA experiments [3] and the HERAFitter analysis framework [4, 5, 3]. The experimental uncertainties were estimated using the MC method [6] and then transformed to eigenvector PDF sets. The new PDF sets were used to study correlations of the Z boson production cross section calculated at NLO and NNLO and to determine theoretical uncertainties for the WW di-boson over Z boson production cross-section ratio. A reduction of the total theoretical uncertainty was observed.

2. PDF analysis

The PDF analysis used the combined HERA data [3]. These input data are accurate measurements of the inclusive deep inelastic scattering (DIS) neutral- and charged-current cross sections combined by the H1 and ZEUS collaborations. The data included in the fit were required to satisfy the $Q^2 > Q^2_{\text{min}} = 7.5\,\text{GeV}^2$ condition in order to stay in the kinematic domain where perturbative QCD calculations can be applied. The theoretical framework was similar to the one used for HERAPDF1.0 [3].

[1] Hereafter referred to as WW

The PDFs for the gluon and quark densities were parameterised at the input scale $Q_0^2 = 1.7\,\mathrm{GeV}^2$ as follows:

$$xg(x) = A_g x^{B_g}(1-x)^{C_g} - A'_g x^{B'_g}(1-x)^{C'_g}; \quad (2.1)$$

$$x\bar{U}(x) = A_{\bar{U}} x^{B_{\bar{U}}}(1-x)^{C_{\bar{U}}}(1+D_{\bar{U}}x+E_{\bar{U}}x^2); \quad (2.2)$$

$$x\bar{D}(x) = A_{\bar{D}} x^{B_{\bar{D}}}(1-x)^{C_{\bar{D}}}; \quad (2.3)$$

$$xu_v(x) = A_{u_v} x^{B_{u_v}}(1-x)^{C_{u_v}}(1+E_{u_v}x^2); \quad (2.4)$$

$$xd_v(x) = A_{d_v} x^{B_{d_v}}(1-x)^{C_{d_v}}(1+D_{d_v}x). \quad (2.5)$$

Here the decomposition of the quark densities follows the one from [5] with $x\bar{U} = x\bar{u}$ and $x\bar{D} = x\bar{d} + x\bar{s}$. The contribution of the s-quark density was coupled to the d-quark density as $x\bar{s} = r_s x\bar{d}$ with $r_s = 1.0$, for fits at all orders, as suggested by [7], and $x\bar{s} = xs$ was assumed. The extra polynomial parameters $D_{d_v}, D_{\bar{U}}, E_{\bar{U}}$ were set to zero for the central fit, however they were allowed to vary to estimate the parameterisation uncertainty. The A_{u_v,d_v} and A_g normalisation were determined by the quark-counting sum rule and momentum sum rule, respectively. The $x \to 0$ behaviour of the u- and d-sea-quark density was assumed to be the same, i.e. $B_{\bar{U}} = B_{\bar{D}}$ and $A_{\bar{U}} = A_{\bar{D}}/(1+r_s)$. The negative term for the gluon density was suppressed at high x by setting $C'_g = 25$. After application of these constraints, the central fit had 13 free parameters.

The data contained statistical, bin-to-bin uncorrelated systematics and 114 correlated systematic uncertainties. The χ^2 per degree of freedom values, χ^2/N_{dof}, for the LO, NLO and NNLO central fits were $523/537$, $500/537$ and $498/537$, respectively.

The PDF uncertainties arising from the experimental uncertainties were estimated using the MC method [6]. A set of 1500 replicas was prepared and used as input for the LO, NLO and NNLO QCD fit. Replicas where one of the fits has failed were discarded. A total of 1337 replicas remained for which fits at all orders had converged and they were used for the further analysis. The distribution of χ^2 values for replicas follows the expectation.

For many applications, the eigenvector representation of the PDF uncertainties is more convenient than the MC representation, since it typically requires fewer PDF sets to describe the uncertainties. A procedure suggested in [8] was adapted to determine the eigenvector representation for the correlated LO and NLO as well as NLO and NNLO MC PDF sets. The covariance matrix of PDFs tabulated on an x grid at the chosen Q_0^2 starting scale was diagonalised, keeping only 39 (45) eigenvectors corresponding to the leading eigenvalues for NLO-NNLO (LO-NLO) sets. The eigenvector representation was found to provide a very good description of the correlation patteren evalued with MC relicas. The correlation among PDF values at different x is shown in Fig. 1. All PDFs show high degree of correlation for neighbouring x values which can be explained by intrinsic smoothness of the PDF parameterisation, which has few parameters, and the fact that the PDFs at comparable x are constrained by similar input data. There is a sizeable anti-correlation between PDFs at small and large x values caused by sum rules. The correlation patterns as a function of x are similar for PDFs determined at NLO and NNLO and, with the exception of the gluon density at high x, there is a strong correlation between NLO and NNLO PDFs.

Model uncertainties in PDFs arise from the uncertainties of the input parameters of the fit. The values of the strange-quark density suppression r_s, the heavy-quark masses M_c and M_b, the strong-coupling constant $\alpha_S(M_Z)$, the Q^2_{min} cut, the starting scale Q_0^2, and parametrisation of PDF shape

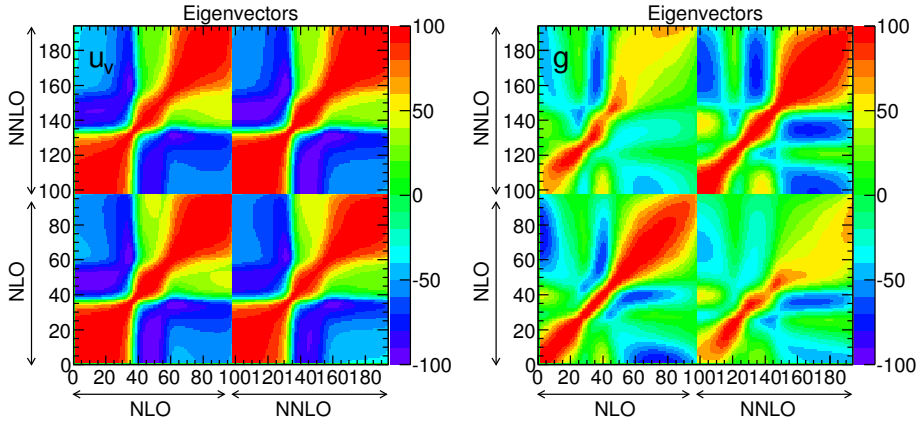

Figure 1: Correlation coefficients, given in percent and represented by different colours, among different PDFs at NLO and NNLO at the starting scale $Q^2 = 1.7$ GeV^2 and x-grid points. The panels show correlation coefficients for $xu_v(x)$ (left) and $xg(x)$ (right) distributions.

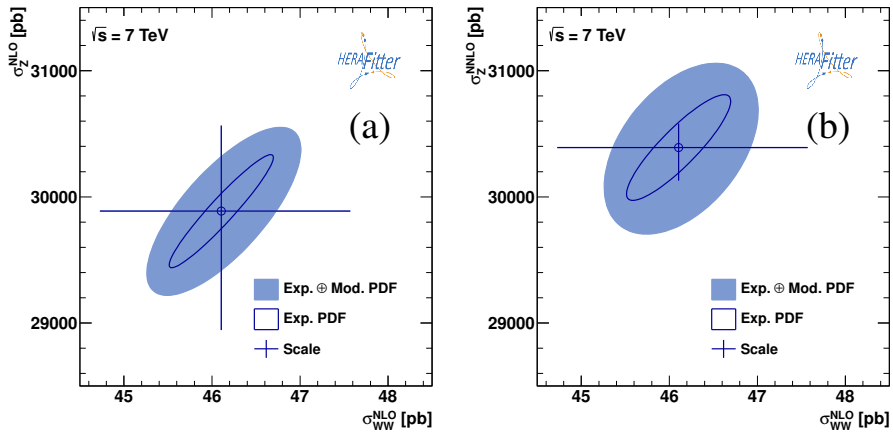

Figure 2: Correlation of the cross-section predictions for WW di-boson production calculated at NLO and Z boson production calculated at NLO (a) and NNLO (b). The error bars indicate scale uncertainties.

were varied. All variations were treated as correlated between differtent orders in the following studies.

3. Predictions for Z and WW production cross sections at the LHC

The usage of the correlated NLO and NNLO PDF sets was exemplified by calculating WW di-boson and Z boson production cross sections for the pp collisions at a $\sqrt{s} = 7$ TeV centre-of-mass energy. The recent measurements of WW di-boson production by the ATLAS and CMS collaborations [9, 1] have generated considerable interest from the theoretical community. The uncertainties of the measurements and predictions are comparable and the measurements are about $1-2\sigma$ above the expectations. The WW di-boson and Z boson production processes are expected

Ratio	Value	Exp. PDF	Mod. PDF	Scale
	$\times 10^{-3}$	$\times 10^{-3}$	$\times 10^{-3}$	$\times 10^{-3}$
$\sigma_{WW}^{\mathrm{NLO}}/\sigma_{Z}^{\mathrm{NLO}}$	1.543	± 0.008	$^{+0.023}_{-0.021}$	$^{+0.069}_{-0.058}$
$\sigma_{WW}^{\mathrm{NLO}}/\sigma_{Z}^{\mathrm{NNLO}}$	1.517	± 0.010	$^{+0.036}_{-0.027}$	$^{+0.050}_{-0.046}$

Table 1: Predictions of the WW di-boson to Z boson production cross-section ratio with PDF and scale uncertainties.

to have similar PDF dependences which may lead to reduced uncertainties for the ratio of the cross sections.

The total cross section for WW di-boson production, σ_{WW}, was calculated at NLO using the MCFM v6.6 program [10, 11]. The contribution from Higgs boson production was not included.

The total cross section for Z/γ^* boson production, σ_Z, was calculated at NLO and NNLO using FEWZ [12, 13]. The invariant mass for the lepton pair was chosen to be $60 < M_{\ell\ell} < 120\,\mathrm{GeV}$ as in the analysis of the CMS collaboration.

Uncertainties due to missing higher-order corrections were estimated by varying the default scales up and down by a factor of two. The scale uncertainty was treated as uncorrelated between WW di-boson and Z boson production.

The correlation of the σ_{WW} and σ_Z cross sections was found to be very large for the experimental PDF uncertainties for both NLO and NNLO calculations. Model and parameterisation PDF uncertainties were also highly correlated for most of the uncertainty sources when both cross sections were calculated at NLO. When σ_Z was calculated at NNLO, an anti-correlation for some sources was observed. In particular, an anti-correlation between σ_{WW} and σ_Z is observed for the variation of the r_s parameter. The M_c, M_b and $\alpha_S(M_Z)$ variations cancel to large extend.

The predicted ratio σ_{WW}/σ_Z using the Z boson production cross sections calculated at NLO and NNLO is given in Table 1. The predictions are compared to the CMS data in Fig. 3. The data and calculations agreed reasonably well. The scale uncertainty was reduced by using σ_Z^{NNLO}. Experimental PDF uncertainties cancel in the ratio becoming negligible compared to the scale uncertainties.

Adding the PDF and scale uncertainties (Table 1) in quadrature, the cross-section ratio of WW di-boson to Z boson production calculated as the NLO ratio was $\sigma_{WW}^{\mathrm{NLO}}/\sigma_Z^{\mathrm{NLO}} = [1.543^{+0.073}_{-0.062}] \times 10^{-3}$ and as the mixed-order ratio was $\sigma_{WW}^{\mathrm{NLO}}/\sigma_Z^{\mathrm{NNLO}} = [1.517^{+0.051}_{-0.047}] \times 10^{-3}$. The usage of the mixed-order calculations led to a 30–40% reduction of the overall theoretical uncertainty.

4. Summary

Sets of LO, NLO and NNLO parton distribution functions are reported preserving the correlations of PDFs determined at different orders. The sets are determined with the HERAFitter program using the combined HERA data. The experimental PDF uncertainties are determined using the MC method and reported using both MC and eigenvector representations. A high degree of correlation is observed for the PDFs at different perturbative order and similar Bjorken x.

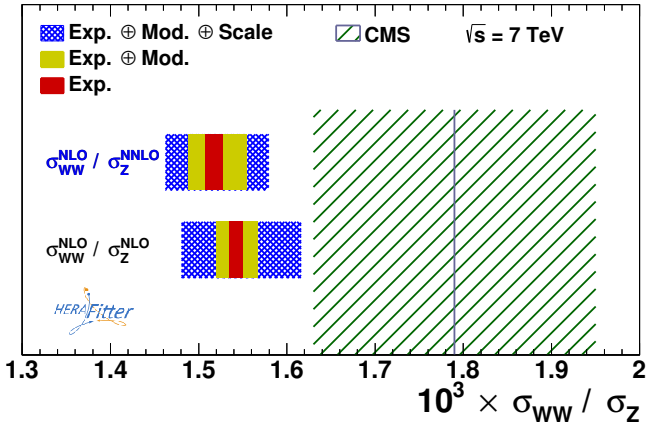

Figure 3: Ratio of the WW di-boson to Z boson production cross sections calculated at NLO and NLO/NNLO compared to the CMS data (hatched area). The inner, middle and outer filled error bars of the predictions indicate experimental and full PDF uncertainties and the total uncertainty calculated as the scale and full PDF uncertainties added in quadrature, respectively.

The correlated NLO and NNLO PDF sets are used to calculate the WW di-boson and Z boson production cross sections. Significant correlations of the PDF uncertainties are observed for the cross sections calculated at different orders. For the ratio of the WW di-boson to Z boson production cross sections an overall 30−40% reduction of uncertainties is observed when using mixed-order calculations due to the reduced higher order uncertainty for the Z boson production cross section calculated at NNLO.

References

[1] CMS Collaboration, Eur.Phys.J. **C73** (2013) 2610 [arXiv:1306.1126].

[2] HERAFitter developers' team and M. Lisovyi, arXiv:1404.4234.

[3] H1 and ZEUS Collaborations, JHEP **1001** (2010) 109 [arXiv:0911.0884].

[4] *HERAFitter, An open source QCD fit framework*, *http://herafitter.org*

[5] H1 Collaboration, Eur.Phys.J. **C64** (2009) 561 [arXiv:0904.3513].

[6] Z. Ajaltouni, S. Albino, G. Altarelli, F. Ambroglini, J. Anderson, *et al.*, Proceedings of the workshop: *HERA and the LHC workshop series on the implications of HERA for LHC physics* [arXiv:0903.3861].

[7] ATLAS Collaboration, Phys.Rev.Lett. **109** (2012) 012001 [arXiv:1203.4051].

[8] J. Gao and P. Nadolsky, arXiv:1401.0013.

[9] ATLAS Collaboration, Phys.Rev. **D87** (2013) 112001 [arXiv:1210.2979].

[10] J. M. Campbell, R. K. Ellis, and C. Williams, JHEP **1107** (2011) 018 [arXiv:1105.0020].

[11] J. M. Campbell, R. K. Ellis, and C. Williams, JHEP **1110** (2011) 005 [arXiv:1107.5569].

[12] C. Anastasiou, L. J. Dixon, K. Melnikov, and F. Petriello, Phys. Rev. **D69** (2004) 094008 [arXiv:hep-ph/0312266].

[13] Y. Li and F. Petriello, Phys.Rev. **D86** (2012) 094034, [arXiv:1208.5967].